ChemComm

Accepted Manuscript

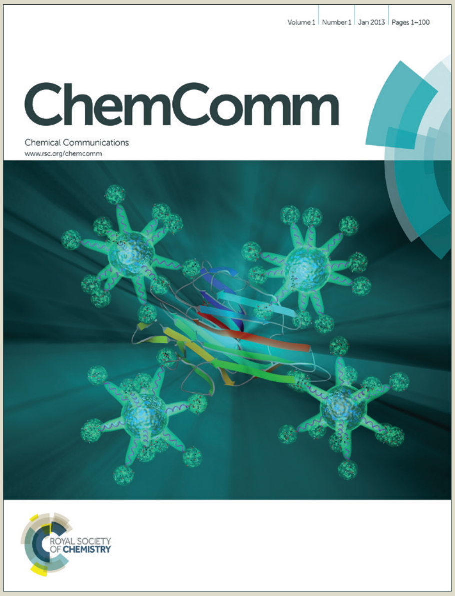

ROYAL SOCIETY OF CHEMISTRY

www.rsc.org/chemcomm

Journal Name

COMMUNICATION

Mg^{2+}-assisted Low Temperature Reduction for Alloyed AuPd/C: Efficient Catalyst for Hydrogen Generation from Formic Acid at Room Temperature

Received 00th January 20xx,
Accepted 00th January 20xx

DOI: 10.1039/x0xx00000x

www.rsc.org/

Shuang Wu[#], Fan Yang[#], Hao Wang, Rui Chen, Pingchuan Sun and Tiehong Chen*

Mg^{2+}-assisted low temperature reduction approach was applied to prepare alloyed AuPd/C nanocatalyst, which exhibited high activity in hydrogen generation from formic acid. At room temperature the initial turnover frequency (TOF) could reach as high as 1120 h^{-1}.

The search for alternative and sustainable energy sources is attracting more and more concern because of the gradual depletion of fossil fuel resources and rising concern of environmental issues.[1] Among the major candidates of renewable energy, hydrogen has been considered as an environment friendly chemical energy carrier with high energy content and wide application in proton exchange membrane fuel cells (PEMFCs).[2] However, classical hydrogen storage methods suffer from weight, cost and safety issues.[3]

As an alternative, chemical hydrogen storage, where hydrogen is released by catalytic decomposition of chemicals rich in hydrogen, such as borohydrides, hydrazine and formic acid (FA), has attracted considerable attention.[4] Formic acid is considered as one of the most promising compounds of hydrogen carrier due to its high hydrogen content, non-toxicity and simplicity to use.[5]

Generally, the decomposition of FA can be achieved via two distinct pathways: dehydrogenation (yielding H_2 and CO_2) and the dehydration (yielding CO and H_2O).[6] The selectivity of pathways was closely related to catalysts, pH values and reaction temperature. Catalysts for decomposition of formic acid include homogeneous catalysts and heterogeneous catalysts. Homogeneous catalysts such as metal (Fe, Pt, Pd, Ni, Ru, Rh, Os, Ir, etc.) complexes with high activity and selectivity have been reported by many research groups.[7-12] Compared to homogeneous catalysts, heterogeneous catalysts have been paid considerable attention in recent years due to the advantages of easy separation and recycled use.

Among heterogeneous catalysts towards the dehydrogenation of formic acid, much attention have been paid to monometallic and polymetallic nanoparticles supported on materials such as ZrO_2, carbon black, graphene oxide, metal-organic framework, macroreticular basic resin, Al_2O_3 and so on,[13-20] with gold,[21-22] palladium[23-28], platinum[16] and other elements[29-34] as active ingredients. Various preparation methods for metallic catalyst have been reported, including vapour deposition, impregnation, co-precipitation, deposition-precipitation, liquid-phase synthesis and so on.[35] Recently, supported AuPd bimetallic catalysts have been applied in decomposition of FA, but their catalytic activities at room temperature need further improvement.[36-40] The development of highly active and selective heterogeneous catalysts for room temperature decomposition of FA is still a challenge for practical use.

As illustrated in literature,[41] the rate of nucleation, growth and aggregation of metal nanoparticles can be well controlled by addition of proper surfactants, polymers, foreign ions, or ligands during the reduction process in solution. Herein, we report a carbon black supported AuPd alloy nanocatalyst prepared by Mg^{2+}- assisted low temperature reduction method. The catalyst exhibited high activity in hydrogen generation from formic acid with an initial turnover frequency (TOF) up to 1120 h^{-1} at room temperature, which is a rather high value for room temperature reaction (Table S1).

A facile Mg^{2+}-assisted low temperature (-3 °C) reduction approach was applied to prepare alloyed AuPd nanoparticles with carbon black as the support and water-ethanol as the solvent (the catalyst was named as Au_6Pd_4-L-Mg, details see Supporting Information). The catalytic performance of the catalysts was evaluated on the basis of the volume of gas generated during the reaction at room temperature (25 °C) (Fig. 1). The as-prepared Au_6Pd_4-L-Mg catalyst showed rather high activity towards hydrogen generation from FA-sodium formate (SF) solution. Within 10 minutes, around 200 ml gas were generated at room temperature (Fig. 1), corresponding to an initial turnover frequency (TOF) of 1120 h^{-1} (at reaction time of 10 min). At reaction time of 20 min the FA conversion was about 50%, corresponding to a TOF of 795 h^{-1}. The activity of as-prepared catalyst was also tested at different reaction temperatures (Fig. 1) and the apparent activation energy

College of Chemistry, School of Materials Science and Engineering, Institute of New Catalytic Materials Science, Key Laboratory of Advanced Energy Materials Chemistry (MOE), Collaborative Innovation Center of Chemical Science and Engineering (Tianjin), Nankai University, Tianjin 300071, PR China.
 # Contribute equally to this work.
E-mail: chenth@nankai.edu.cn

Electronic Supplementary Information (ESI) available: [experimental details and characterization results]. See DOI: 10.1039/x0xx00000x

(Ea) (Fig. S1) was calculated to be 18.5 kJ/mol, which is relatively low compared to activation energies reported in earlier literature (Table S2). By gas chromatography (GC) the concentration of CO in the reforming gas was around 100 ppm (Fig. S2 and Fig. S3).

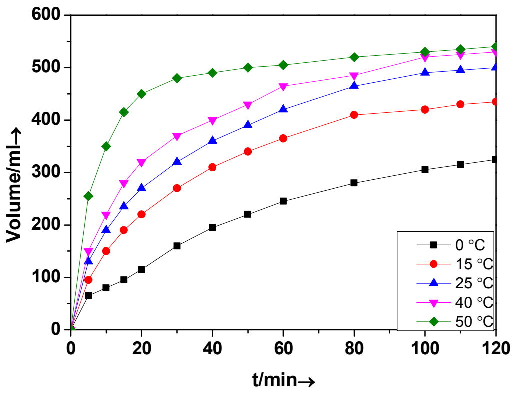

Fig. 1 Gas generation with Au$_6$Pd$_4$-L-Mg at different reaction temperatures from FA/SF (sodium formate) (10 ml, 1.1 M FA, 4.0 M SF) solution.

The X-ray diffraction (XRD) pattern (Fig. S4) of Au$_6$Pd$_4$-L-Mg showed that the nanoparticles exhibit the fcc structure of metallic Au. As the relative difference of the atom radii of Au (0.144 nm) and Pd (0.138 nm) is 4.2% (lower than 15%), Pd can be incorporated into Au lattice to form fcc structure based on Hume-Rothery rule.[30] As shown in Fig. S4, compared with the XRD pattern of pure Au supported on carbon black, the characteristic peak of Au in Au$_6$Pd$_4$-L-Mg was widened and the strength decreased due to the formation of Au-Pd alloy and smaller particle size. When Au$_6$Pd$_4$-L-Mg was thermally treated via reduction by H_2 at 300 °C (details see Supporting Information), the intensity of the Au (111) diffraction peak increased (Fig. S5) due to annealing effect of the AuPd alloy.[42] The slight shift of the Au (111) peak to higher degree could be due to the incorporation of Pd within Au lattice. Meanwhile the absence of Pd(111) diffraction also indicated the formation of AuPd alloy.

The AuPd alloy formation could also be proved by UV-vis spectroscopy. Because carbon black is not suitable for UV-vis spectroscopy, Al_2O_3 was selected as support and Au/Al_2O_3, Pd/Al_2O_3 and Au$_6$Pd$_4$/Al_2O_3 were prepared, respectively. For Au/Al_2O_3, in the UV-vis spectrum (Fig. S6) there was an obvious plasmon absorption band at 520 nm, while in the spectrum of Au$_6$Pd$_4$/Al_2O_3, the band disappeared. This indicated again that Au and Pd formed alloyed structure without isolated Au nanoparticles.[43]

The transmission electron microscopy (TEM) images of the as-prepared Au$_6$Pd$_4$-L-Mg are shown in Fig. 3. The nanoparticles are well dispersed on the carbon black support with average particle size of around 2~3 nm. The energy dispersive X-ray spectrometry (EDS) on one nanoparticle proves the coexistence of both Au and Pd elements (Figure S7a). By EDS the ratio of Au and Pd is roughly 6:4, which is consistent with the initial content of Au and Pd in the precursor. The STEM-EDS line-scan profile of one AuPd alloy nanoparticle showed that Au and Pd coexisted and homogeneously distributed in the particle, indicating the formation of AuPd alloy structure. (Fig. 3e), which is consistent with the result of element mapping (Figure S7b). The content of Au and Pd was also determined by inductively coupled plasma-atomic emission spectrometry (ICP-AES) (Table S3). The metal content of Au$_6$Pd$_4$-L-Mg catalyst is consistent with the result of EDS.

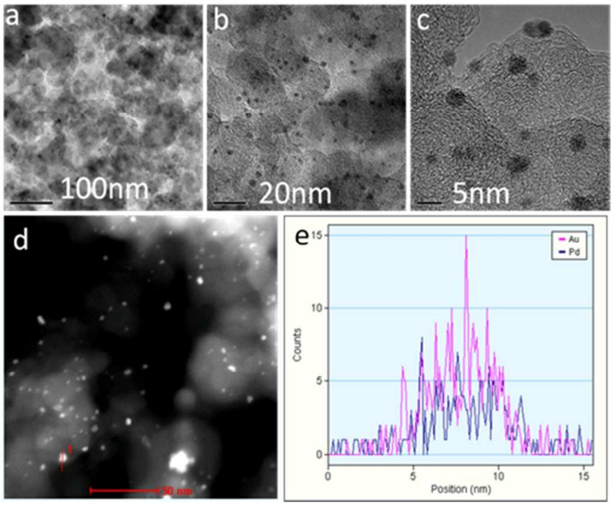

Fig.2 TEM images of Au$_6$Pd$_4$-L-Mg (a, b and c) and STEM-EDS line-scan profile of one AuPd nanoparticle(d and e).

The Au:Pd ratio also played important role in activity of the alloyed catalysts. As shown in Fig. S8, pure Au/C catalyst showed no activity towards dehydrogenation of formic acid. The activity of pure Pd/C catalyst was greatly increased by formation of AuPd alloy with proper Au:Pd ratio, and when the ratio of Au and Pd was 6:4, the catalyst exhibited the best performance.

Low temperature reduction (-3 °C) is very important for the catalyst preparation. For comparison, catalyst was also prepared by reduction at room temperature (named as Au$_6$Pd$_4$-R), and the XRD patterns of Au$_6$Pd$_4$-L-Mg, Au$_6$Pd$_4$-L (low temperature reduction but without addition of Mg^{2+}) and Au$_6$Pd$_4$-R were shown in Fig. S9. The sharper and higher Au (111) diffraction peak for Au$_6$Pd$_4$-R indicated relatively larger particle size of AuPd alloy nanoparticles, and this point was also shown in TEM images (Fig. S10). TEM images of Au$_6$Pd$_4$–R (Fig. S10) showed relatively severe aggregation and the size of some large aggregated particles could even reach 100 nm. Au$_6$Pd$_4$-R showed particularly low activity for the decomposition of formic acid, with only 100 ml gas generated for two hours. For the catalyst prepared at -3 °C, Au$_6$P$_4$-L exhibits an obvious improvement in catalytic activity (Fig. S11). The reduction process at lower temperature could efficiently slow down the nucleation and aggregation of noble metal nanoparticles,[44, 45] which would leads to smaller nanoparticles with larger surface area available for the reactants.

As reported in literature, the process of nucleation and growth for bimetallic nanocatalyst could be regulated by adding foreign ions.[41] Here in our case, the presence of Mg^{2+} in the synthesis process at -3 °C could further exert control to nucleation of AuPd alloy nanoparticles and this could induce further improvement in activity of Au$_6$Pd$_4$-L-Mg compared with that of Au$_6$Pd$_4$-L (Fig. S11). To further determine the influence of Mg^{2+} on their nucleation and growth process of metal particles, the effect of Mg^{2+} on formation of Pd nanoparticles was studied. The activity of Pd/C prepared in the presence of Mg^{2+} show obvious improvement compared to that synthesized without Mg^{2+} addition (See Fig. S12). As shown in the TEM images, with the addition of Mg^{2+}, the size of Pd nanoparticles was generally smaller than those synthesized without Mg^{2+} (See Fig. S13). A series of Au_6Pd_4-L-Mg catalysts were also prepared with different concentrations of Mg^{2+} and their catalytic activities gradually increased with the concentration of Mg^{2+} (Fig. S14). However, the activity decreased with further increasing of Mg^{2+}. During the reduction process, Mg^{2+} could react with sodium borate (the product of the decomposition of $NaBH_4$) to produce $Mg_2B_2O_5$, which is only partially soluble in the solution. Too much Mg^{2+} would induce the formation of $Mg_2B_2O_5$ precipitate, which would also act as support and disturb the dispersion of AuPd nanoparticles on carbon black. Since the synthesized catalyst was washed with both water and ethanol, there are only traces of magnesium left in the catalyst, as shown by the results of ICP and EDS.

After catalytic reaction the catalyst was recollected and dried for recycled runs. As shown in Fig. 5, recycled catalysts showed similar activity as newly prepared catalysts in the second and third run, taking into account a little loss of catalyst in the recycling process. The structure of Au_6Pd_4-L-Mg catalyst is stable during the reaction as seen in the TEM images of recycled catalyst (Fig. S15).

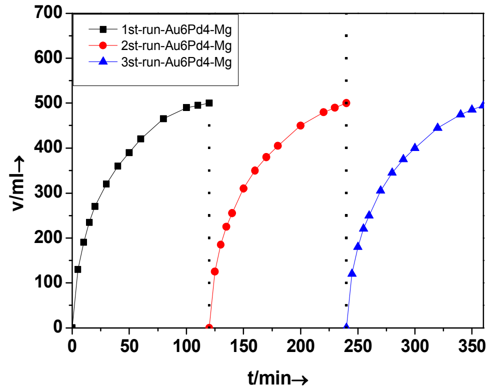

Fig.3 Gas generation with Au_6Pd_4-L-Mg at sequential runs at room temperature from FA/SF (1.1 M FA, 4.0 M SF).

In summary, Mg^{2+}-assisted low temperature reduction approach was used to prepare alloyed AuPd/C nanocatalyst. Relatively higher dispersion and smaller size of the AuPd alloy nanoparticles were obtained by reduction at -3 °C in the presence of Mg^{2+}. The catalyst showed high activity in the hydrogen generation from formic acid, and the initial turnover frequency (TOF) reached 1120 h^{-1} at room temperature. Meanwhile, the Mg^{2+}-assisted low temperature synthetic method could provide a new route for the synthesis of supported metal nanoparticles catalyst.

This work was supported by NSFC (No. 21373116 and 21421001), the Tianjin Natural Science Research Fund (13JCYBJC18300), RFDP (20120031110005), and the MOE Innovation Team (IRT13022) of China.

Notes and references

1 V. G. Dovì, F. Friedler, D. Huisingh and J.J. Klemeš, *J. Clean. Prod.*, 2009, **17**, 889.
2 Y. Li, H. Chen, X. Zhang, C. Tan and Y. Ding, Appl. *Therm. Eng.*, 2010, **30**, 1985.
3 a) M. Felderhoff, C. Weidenthaler, R. V. Helmolt and U. Eberle, *Phys. Chem. Chem. Phys.*, 2007, **9**, 2643; b) A. F. Dalebrook, W. Gan, M. Grasemann, S. Moret and G. Laurenczy, *Chem. Commun.*, 2013, **49**, 8735.
4 M. Yadav and Q. Xu, *Energy Environ. Sci.*, 2012, **5**, 9698.
5 a) M. Grasemann and G. Laurenczy, *Energy Environ. Sci.*, 2012, **5**, 8171; b) M. G. Mura, L. D. Luca, G. Giacomelli and A. Porcheddu, *Adv. Synth. Catal.*, 2012, 354, 3180; c) B. Loges, A. Boddien, F. Gärtner, H. Junge and M. Beller, *Top. Catal.*, 2010, **53**, 902.
6 a) K. Jiang, H. Zhang, S. Zou and W. Cai, *Phys. Chem. Chem. Phys.*, 2014, **16**, 20360.b) J. Wang, H. Zhang, K. Jiang and W. Cai, *J. Am. Chem. Soc.*, 2011, **133**, 14876.
7 a)A. Boddien, B. Loges, H. Junge and M. Beller, *ChemSusChem*, 2008, **1**, 751.b) H. Junge, A. Boddien, F. Capitta, B. Loges, J. R. Noyes, S. Gladiali and M. Beller, *Tetrahedron Lett.*, 2009, **50**, 1603.
8 C. Johnson, D. J. Morris and M. Wills, *Chem. Soc. Rev.*, 2010, **39**, 81.
9 B. Loges, A. Boddien, H. Junge and M. Beller, *Angew. Chem. Int. Ed.*, 2008, **47**, 3962.
10 A. Boddien, B. Loges, H. Junge, F. Gärtner, J. R. Noyes and M. Beller, *Adv. Synth. Catal.*, 2009, **351**, 2517.
11 A. Boddien, D. Mellmann, F. Gartner, R. Jackstell, H. Junge, P. J. Dyson, G. Laurenczy, R. Ludwig and M. Beller, *Science*, 2011, **333**, 1733.
12 S. Fukuzumi and T. Suenobu, *Dalton T.*, 2013, **42**, 18.
13 Q. Y. Bi, X. L. Du, Y. M. Liu, Y. Cao, H. Y. He and K. N. Fan, *J. Am. Chem. Soc.*, 2012, **134**, 8926.
14 Z. L. Wang, J. M. Yan, H. L. Wang, Y. Ping and Q. Jiang, *Sci. Rep.*, 2012, **2**.
15 D. A. Bulushev, S. Beloshapkin and J. R. H. Ross, *Catal. Today*, 2010, **154**, 7.
16 F. Solymosi, Á. Koós, N. Liliom and I. Ugrai, *J. Catal.*, 2011, **279**, 213.
17 Y. Ping, J. M. Yan, Z. L. Wang, H. L. Wang and Q. Jiang, *J. Mater. Chem. A*, 2013, **1**, 12188.
18 X. Gu, Z. H. Lu, H. L. Jiang, T. Akita and Q. Xu, *J. Am. Chem. Soc.*, 2011, **133**, 11822.
19 K. Mori, M. Dojo and H. Yamashita, *ACS Catal.*, 2013, 3, 1114.
20 M. Ojeda and E. Iglesia, *Angew. Chem. Int. Ed.*, 2009, **48**, 4800.
21 A. Gazsi, T. Bánsági and F. Solymosi, *J. Phy. Chem. C*, 2011, **115**, 15459.
22 M. Yadav, T. Akita, N. Tsumori and Q. Xu, *J. Mater. Chem.*, 2012, **22**, 12582.
23 M. Yadav, A. K. Singh, N. Tsumori and Q. Xu, *J. Mater. Chem.*, 2012, **22**, 19146.
24 X. Wang, G. W. Qi, C. H. Tan, Y. P. Li, J. Guo, X. J. Pang and S. Y. Zhang, *Int. J. Hydrogen Energy*, 2014, **39**, 837.
25 C. Hu, J. K. Pulleri, S. W. Ting and K. Y. Chan, *Int. J. Hydrogen Energy*, 2014, **39**, 381.
26 D. A. Bulushev, L. Jia, S. Beloshapkin and J. R. H. Ross, *Chem. Commun.*, 2012, **48**, 4184.
27 S. Jones, J. Qu, K. Tedsree, X. Q. Gong and S. C. E. Tsang, *Angew. Chem. Int. Ed.*, 2012, **51**, 11275.
28 Q. L. Zhu, N. Tsumori and Q. Xu, *Chem. Sci.*, 2014, **5**, 195.
29 A. Bulut , M. Yurderi, Y. Karatas, M. Zahmakiran, H. Kivrak and M. Gulcan , *Appl. Catal.* B, 2015,**164**, 324
30 Z. L. Wang, J. M. Yan, Y. Ping, H. L. Wang, W. T. Zheng and Q. Jiang, *Angew. Chem. Int. Ed.*, 2013, **52**, 4406.

31 a)S. Zhang, Ö. Metin, D. Su and S. Sun, *Angew. Chem. Int. Ed.*, 2013, **52**, 3681. b) K. Tedsree, T. Li, S. Jones, C. W. A. Chan, K. M. K. Yu, P. A. J. Bagot, E. A. Marquis, G. D. W. Smith and S. C. E. Tsang, *Nat. Nanotechnol.*, 2011, **6**, 302.
32 C. Hu, S. W. Ting, J. Tsui and K. Y. Chan, *Int. J. Hydrogen Energy*, 2012, **37**, 6372.
33 Y. l. Qin, J. Wang, F. Meng, L. Wang and X. Zhang, *Chem. Commmun.*, 2013, **49**, 10028.
34 K. Jiang, K. Xu, S. Zou and W. B. Cai, *J. Am. Chem. Soc.*, 2014, **136**, 4861.
35 Z. Wei,J. Sun, Yan Li,A. K. Datye and Y. Wang, *Chem. Soc. Rev.*, 2012, **41**, 7 994.
36 X. Zhou, Y. Huang, C. Liu, J. Liao, T. Lu and W. Xing, *ChemSusChem*, 2010, **3**, 1379.
37 X. Zhou, Y. Huang, W. Xing, C. Liu, J. Liao and T. Lu, *Chem. Commun.*, 2008, 3540.
38 Y. Huang, X. Zhou, M. Yin, C. Liu and W. Xing, *Chem. Mater.*, 2010, **22**, 5122.
39 Z. L. Wang, J. M. Yan, H. L. Wang, Y. Ping and Q. Jiang, *J. Mater. Chem. A*, 2013, **1**, 12721.
40 S. Wu, F. Yang, P. Sun and T. Chen, *RSC Adv.*,2014, **4**, 44500
41 D. Wang and Y. Li, *Adv. Mater.*, 2011, **23**, 1044.
42 N. Dilshad, M. S. Ansari, G Beamson and D. J. Schiffrin, *J. Mater. Chem.*, 2012, **22**, 10514.
43 M. Mandal, S. Kundu, S. K. Ghosh and T. Pal, *J. Photoch. Photobio. A*, 2004, **167**,17.
44 P. Chen, L. Guo and Y. Wang, *J. Power Sources*, 2013, **222**, 52 6.
45 G. T. Cardenas, J. K. Klabunde and B. E. Dale, *Langmuir*, 1987, **3**, 986.

Colour graphic

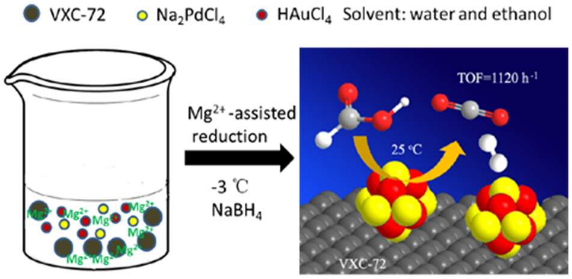

Alloyed AuPd/C nanocatalyst was prepared via Mg^{2+}-assisted low temperature reduction, and exhibited high activity in room temperature decomposition of formic acid.